

Rotational optomechanical cooling of a nanofiber torsional modes

Dianqiang Su^{1,2}, Pablo Solano^{3,4}, Luis A. Orozco⁵, Yanting Zhao^{1,2}

¹*State Key Laboratory of Quantum Optics and Quantum Optics Devices, Institute of Laser Spectroscopy, Shanxi University, Taiyuan 030006, People's Republic of China.*

²*Collaborative Innovation Center of Extreme Optics, Shanxi University, Taiyuan 030006, People's Republic of China.*

³*Department of Physics and Research Laboratory of Electronics, Massachusetts Institute of Technology, Cambridge, Massachusetts 02139, USA.*

⁴*Departamento de Física, Universidad de Concepción, Casilla 160-C, Concepción, Chile.*

⁵*Joint Quantum Institute, Department of Physics and NIST, University of Maryland, College Park, MD 20742, USA.*

Linearly polarized light can exert a torque on a birefringent object when passing through it. This phenomena, present in Maxwell's equations, was revealed by Poynting¹ and beautifully demonstrated in the pioneer experiments of Beth^{2,3} and Holbourn⁴. Modern uses of this effect lie at the heart of optomechanics with angular momentum exchange between light and matter⁵⁻⁹. A milestone of controlling movable massive objects with light is the reduction of their mechanical fluctuations, namely cooling. Optomechanical cooling has been implemented through linear momentum transfer of the electromagnetic field in a variety of systems¹⁰⁻¹³, but remains unseen for angular momentum transfer to rotating objects. We

present the first observation of cooling in a rotational optomechanical system. Particularly, we reduce the thermal noise of the torsional modes of a birefringent optical nanofiber, with resonant frequencies near 200 kHz and a Q-factor above 2×10^4 ¹⁴⁻¹⁶. Nanofibers are centimeter long, sub-micrometer diameter optical fibers that confine propagating light, reaching extremely large intensities ^{17,18}, hence enhancing optomechanical effects. The nanofiber is driven by a propagating linearly polarized laser beam. We use polarimetry of a weak optical probe propagating through the nanofiber as a proxy to measure the torsional response of the system. Depending on the polarization of the drive, we can observe both reduction and enhancement of the thermal noise of many torsional modes, with noise reductions beyond a factor of two. The observed effect opens a door to manipulate the torsional motion of suspended optical waveguides in general, expanding the field of rotational optomechanics, and possibly exploiting its quantum nature for precision measurements in mesoscopic systems.

The idea of using light as noise tranquilizer for Fabry-Perot interferometers ¹⁹ has had a major influence on the development of optomechanics on the micro and nano scale ¹³, with remarkable implementations for LIGO ²⁰. The reduction of thermally induced noise in the displacement of a mechanical object by controlling its interaction with light is known as optomechanical cooling. So far, all experimental realizations of it rely on the transfer of linear momentum between light and an object ²¹⁻²³. The transfer of angular momentum has applications in several systems, by means of light polarization ²⁴ or orbital angular momentum ²⁵, but it has not been used to reduce the mechanical fluctuations of a rotational oscillator. To enable such optomechanical effect, one benefits from lightweight objects and large optical intensities. Currently, small optical waveguides ²⁶ highly con-

fine the spatial modes of propagating light. This could lead in the future to suspended waveguides that experience torsion as good candidates for rotational optomechanics. In particular, rotational optomechanical coupling has already been observed in optical nanofiber (ONF) waveguides ¹⁶.

An ONF waveguide is a macroscopic object along one direction and nanometric in the transverse dimensions (see Fig. 1a). It generally has vibrational, compressional, and torsional modes ¹⁵. Here we focus on the torsional ones, with angular momentum oscillating along the long axis. The thermally induced internal molecular vibrations of the ONF set the torsional modes in motion, visible only in vacuum since a surrounding gas damps the oscillations ¹⁴. We are interested in modifying the oscillation of such torsional modes by applying a torque with guided light. The optomechanical effect is proportional to the intensity of the guided field, which for 1 mW of power is greater than 10^8 mW/cm². This allows us to observe small torsionally induced differences in the index of refraction, which are estimated to be in the 10^{-8} range, on top of the stress induced ones that are close to 10^{-3} ¹⁵.

For simplicity, we model the nanofiber as a thick birefringent disk, an approximation that allows us to gain intuition and extract physically relevant features of the system (see Methods). The torque applied to a polarizable medium is $\vec{T} = \vec{P} \times \vec{E}$, where \vec{P} is the polarization of the medium and \vec{E} is the electric field in the medium. Such torque is a function of the angle between the electric field and the optical axis $\theta(t)$ as^{3,6}:

$$T(t) = \frac{\epsilon E^2}{2\omega_1} \sin \Gamma \sin 2\theta(t), \quad (1)$$

where ϵ is the electric permittivity related to the effective index of refraction of the ONF, E is

the amplitude of the electric field of the drive, ω_l is the laser frequency, and $\Gamma = kd(n_o - n_e)$ with k the wavenumber, d the dielectric thickness, and n_o and n_e the ordinary and extraordinary indices of refraction. The equation of motion that describes the system is the one for a rotational harmonic oscillator with a driving force of the form of Eq. (1) (see Methods for details). Taking the small angle approximation, the linear term $2\theta(t)$ can be treated as an effective modification of the spring constant of the torsional mode, which can be positive or negative depending of the light polarization angle. The spectral density for a small perturbation of the rotation angle $\delta\theta$, around a fix value θ , in the vicinity of one of its torsional resonances, is (see Methods)

$$S_{\delta\theta}(\omega) = \frac{4k_B T \gamma}{((\kappa - A_0 \cos 2\theta) - I\omega^2)^2 + \gamma^2 \omega^2}, \quad (2)$$

where k_B is the Boltzmann constant, T is the absolute temperature, γ is the damping coefficient, κ is the torsional spring constant, I is the moment of inertia, and $A_0 = \frac{\epsilon E^2}{2\omega_l} \sin \Gamma$ is the amplitude of the applied optical torque. The noise in Eq. (2) can increase or decrease depending on the polarization angle of a guided field with respect to the optical axis of the ONF waveguide. This effect allows for a reduction of the roto-mechanical fluctuations by an optomechanical coupling.

Our apparatus, schematically drawn in Fig. 1, operates at room temperature. Given the geometry of our ONF, the frequency of the first torsional mode lies near 200 kHz^{14,16}. We record the spectral density around the resonances in order to study their thermal excitation. We use a linearly polarized weak probe, with negligible optomechanical effects ($<60 \mu\text{W}$), propagating through the ONF as a proxy to measure the nanofiber rotation. We monitor its polarization rotation measuring both linear components with a balanced photodetector (BPD) to filter common noise and drifts (see Fig. 1b). The photocurrent is linearly proportional to the ONF rotation angle, so the mechanical

noise is measured through the power spectrum from the photocurrent of the BPD. Yet, it is hard to estimate the actual rotation angle of the ONF from the signal (see Methods). The ONF has its first torsional mode at about 189.7 kHz with a full width at half maxima (FWHM) of 7 Hz, corresponding to a $Q \sim 2.7 \times 10^4$.

The optomechanical coupling is enabled by propagating an external drive laser through the ONF waveguide. We can selectively excite each torsional mode by modulating the amplitude of the linearly polarized drive laser at the appropriate polarization angle, in a similar way to Fenton *et al.*¹⁶, where the amplitude of a driven torsional mode could increase by as much as 40 dB over the thermally driven excitations. When the linearly polarized drive is kept on at a non-zero polarization angle relative to the ONF optical axis, it can exert a torque on the nanofiber, which will consequently rotate, changing the relative angle to a new equilibrium position. The optomechanically modified rotational potential around the new equilibrium position could be more or less stiff depending on the relative angle between the drive and the ONF optical axis. This bi-directional optomechanical coupling can lead to a reduction or enhancement of the thermally driven rotation of the ONF around the equilibrium position, meaning cooling or heating.

Figure 2 shows measurements of the thermal noise on resonance as a function of the drive polarization angle for the first torsional mode. This mode is signaled with an arrow in the inset of Fig. 2 for comparison with higher order ones. The amplitude of the noise follows well the prediction of the theoretical model, represented by a green continuous line in the figures (see Methods). Figure 2a has a driving power of 1.5 mW. For higher powers, starting at 2 mW, we

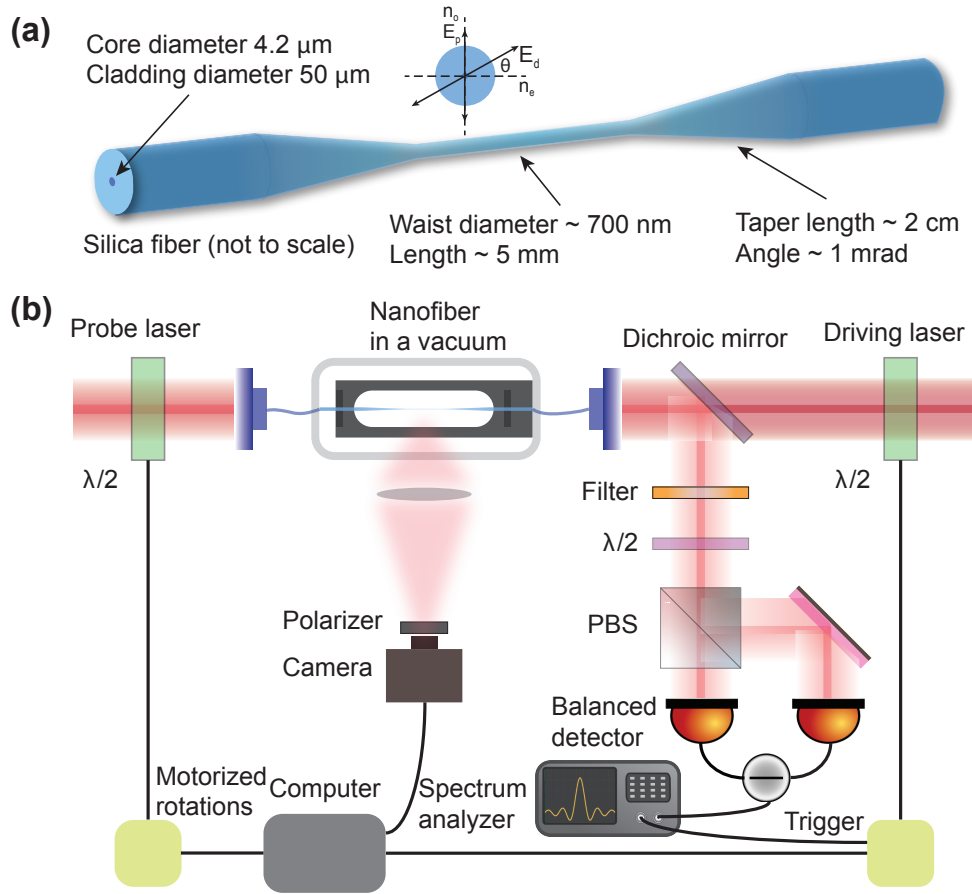


Figure 1: (a) Schematic of an ONF with two effective polarization axes associated with an ordinary (O) and an extraordinary (E) indices of refraction forming a relative angle θ with the input light polarization. The fiber is produced with the heat and pull method²⁷ with no specified birefringence. The 700 nm diameter of the nanofiber allows the propagation of the fundamental HE_{11} mode and some higher order modes²⁸ for the used frequencies. (b) Schematic of the apparatus. The nanofiber resides in a vacuum chamber. There is a side window to monitor the Rayleigh scattering with a polarizer and a camera. The image region of interest encompasses the waist of the ONF and we analyze the signal to guarantee mostly linearly polarized light in the waist region²⁹. We operate with two wavelengths, a probe and a drive laser of 852 nm and 780 nm wavelength respectively. Both are counterpropagating beams with independent polarization control by motorized half-waveplates. The drive laser enters through a dichroic mirror. The probe exiting the ONF passes through an interference filter to suppress any light from the drive beam, followed by another waveplate to carefully adjust the power ratio at the output of a polarizing beam splitter that separates the light into two polarizations components. The two outputs then go to a balanced photodiode pair to extract the difference and amplify it. The signal then goes to a spectrum analyzer and is transferred to a computer for further processing and analysis.

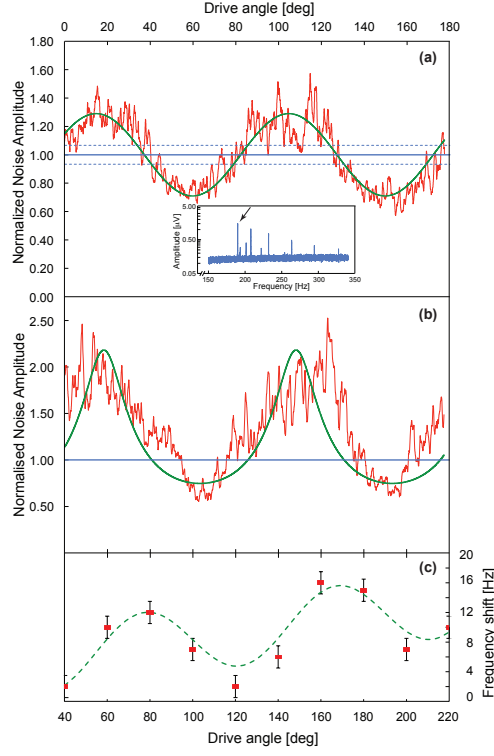


Figure 2: Reduction of the thermal fluctuations of the first torsional mode of an optical ONF as we scan by 180° the motor-controlled drive waveplate, which triggers the spectrum analyzer. The solid green lines are the expected behaviors (see Methods, Eq. (13)). **(a)** Ratio of the driven amplitude noise with respect to the undriven noise for a drive power of 1.5 mW, with a resonant frequency of 190.260 kHz. The dashed green lines bound represents (\pm one standard deviation) the thermal noise level (mean $7.5 \mu\text{V}$) over a similar time span to the data taking. The angle of the probe is set with a half-waveplate at 50.6° , as the drive polarization scans 180° (top axis). The power spectrum in the inset shows a comparison of the first torsional mode (shown by the arrow) to the higher order ones. **(b)** Ratio of the driven amplitude noise with respect to the undriven noise for a drive power of 2 mW, with a resonant frequency of 190.688 kHz. The angle of the probe is set with a half-waveplate at 5.6° , as the drive polarization scans 180° starting at 40° (bottom axis). **(c)** Frequency shift of the resonance at 190.688 kHz as a function of drive polarization angle. All parameters are the same as in **(b)**. The dashed green line is the expected sinusoidal behavior (see Methods, Eq. (12)), allowing for a slow drift in the resonant frequency of 0.04 Hz/deg, consistent with normally observed experimental drifts.

observe an asymmetry in the noise as a function of the drive angle, clearly visible in Fig. 2b. Defining the asymmetry in the noise A as the ratio of the increased versus the decreased noise amplitude we find that for a 1.5 mW drive $A = 1 \pm 0.2$ and for a 2 mW drive $A = 2.4 \pm 0.2$, where the errors are estimates of the standard deviation based on the peak to peak excursions around the extrema. The asymmetry arises from the non-linear dependence of the noise to the optomechanically modified torsional spring constant (see Methods). Fig. 2c shows the position of the resonance as a function of the angle of the drive laser, under very similar conditions as b. We expect a frequency shift as a function of the drive polarization angle, together with noise amplitude change (see Methods, Eq. (12)). The measurement is sensitive to the small power changes as a function of the drive angle, which thermally induce changes of the resonant frequency, preventing us from making quantitative assessments.

The optomechanical coupling has a period of 180° with respect to the polarization angle of the drive, as shown by Eq. (1), twice the half-waveplate angle in Fig. 2. The probe beam signal has a period of 90° , since the polarization analysis is proportional to the square of the polarization rotation sinusoidal function, as described by Malus's law. We observe that phase of the periodic modulation of the noise amplitude as a function of the drive polarization angle is a function of the probe polarization angle. Fig. 2a and b are shown at probe angles differing by 90° , and the signal as a function of drive polarization angle is correspondingly shifted by 90° . We theorize that non-linear optical effects, such as Kerr, between the probe and the nanofiber can change the local index of refraction adding to the stress-induced birefringence. This suggests that light-induced birefringence can be used for better engineering and control of the spin-optomechanical coupling,

instead of relying on naturally caused birefringences.

Figure 3 shows the normalized thermal noise reduction as we increase the drive power. The power dependence of the noise reduction seems to decrease for high drive powers, in accordance with the prediction shown by the green line (see Methods, Eq. (13)). For the range of driving powers available in our experiment, we observe up to a factor of two reduction in the thermal noise of the fundamental torsional mode. We found that at higher powers (>10 mW), the mechanical stability of the ONF appears compromised. We observe large fluctuations on the Rayleigh light scattered out of the nanofiber, suggesting that vibrational, violin, modes are excited.

We observe that all higher order torsional modes decrease their amplitudes, some by more than factor of two. Inset **b** of Fig. 3 shows an example of this, demonstrating that the optomechanical coupling is broadband, affecting all modes simultaneously. This characteristic is quite different from typical optomechanical cooling protocols that tend to rely on a narrow bandwidth and driving almost on-resonance¹³.

A torsional mode can be selectively driven by a periodic modulation of the amplitude of drive¹⁶. We observe hysteresis in the amplitude of the oscillation when sweeping the modulation frequency of the drive in opposite direction, heralding many more studies of the non-linear dynamics that may include bistabilities. Atomic optical dipole traps in nanofibers can benefit from the shown mechanisms to quiet torsional modes with frequencies comparable to trapping frequencies³⁰. In order to observe quantum effects, the mechanical system has to be at a temperature $T < (f \times Q)h/k_B$ ³¹. Although in our case this corresponds to $T < 0.3$ K, it should be possible

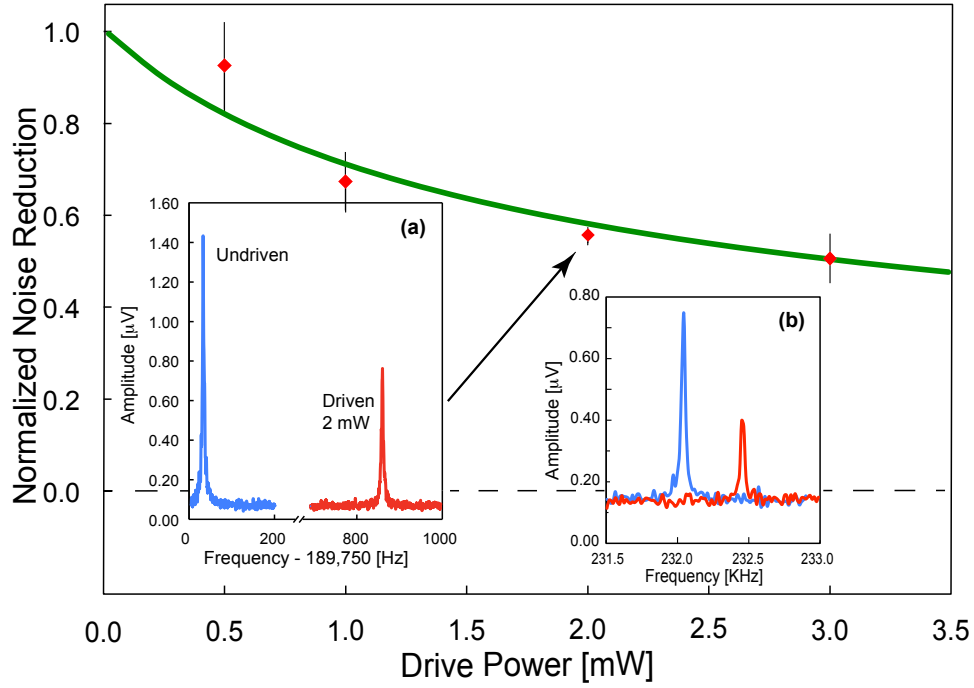


Figure 3: Ratio of the rotational noise amplitudes with and without drive as a function of drive power for a drive angle that minimizes the noise and a fixed probe angle. The error bars are the standard deviation of the mean. The green line is the functional form of the minimum of the amplitude of the noise (see Methods, Eq. (13)). The black dashed line indicates the zero ratio amplitude. Inset (a) shows the power spectrum of the first torsional mode resonance in the undriven (blue) and driven (red) cases. The horizontal axis is broken and most of the shift observed is thermal. The amplitude reduction of the noise is consistent with the 2 mW point in the graph. Inset (b) shows the undriven (blue) and driven (red) resonances for a higher order torsional mode around 232 kHz at the same drive power, showing greater suppression than the fundamental mode.

to design and fabricate suspended optical waveguides with higher-frequency torsional modes and higher Q -factor for reaching the quantum limit at experimentally achievable temperatures. One can envision the engineering of suspended optical waveguides with transverse long arms to create torsional pendula³². A transverse asymmetry of the waveguide could allow for a strong rotational optomechanical coupling suitable for a reduction of thermal and quantum noises, bringing a new tools to precision measurements at the nanoscale.

Acknowledgments

We are grateful to for useful discussions with Nergis Mavalvala and Howard J. Carmichael. L. A. O. thanks the hospitality of the Institute of Laser Spectroscopy, Shanxi University, China, where this experiment has been performed. This work was supported by National Key R&D Program of China (Grant No. 2017YFA0304203), Natural Science Foundation of China (Nos. 61675120, 11434007, 61875110), Natural Science Foundation of China Project for Excellent Research Team (No. 61121064), Shanxi '1331 Project' Key Subjects Construction, PCSIRT (No. IRT_17R70) and 111 project (Grant No. D18001) from China, and [conicyt-pai 77190033](#) from Chile.

Author Contributions

D. S., L. A. O., and Y. Z. conceived the project. D. S. and L. A. O. realized the measurements. L. A. O. and P. S. developed the theoretical model. All authors discussed the results, contributed to the data analysis and worked together on the manuscript.

Author Information

The authors declare no competing financial interests. Correspondence and requests for materials should be addressed to Y. Z.(zhaoyt@sxu.edu.cn).

Methods

Experimental methods A tapered single mode ONF, with waist of 350 ± 20 nm radius and 5 mm length, is put inside a vacuum chamber. The ONF is made by the heat-and-pull method following the algorithm in Ref. ²⁷, using a stripped down commercial optical fiber: Fibercore, SM1500 (4.2 μ m core diameter, 50 μ m cladding diameter).

These ONFs offer tight optical mode confinement (less than the wavelength of light) and diffraction-free propagation. The glass malleability ensures low surface roughness. The smoothness of the surface is a great asset since it leads to ultra-high transmission structures that can withstand high optical intensities. We analyze the light (Rayleigh scattering) out at the waist region with a rotatable polarizer and a camera ²⁹. The polarization contrast of the Rayleigh scattering is typically 20%, mostly due to background scattering of light in the vacuum chamber. We do not see significantly brighter points on the image which, together with the good optical transmission, ensures that no particles have significantly spoiled the nanofiber performance.

We use the fundamental guided mode of light propagating through the ONF, with zero orbital angular momentum, for both drive and probe lasers. Although our ONF allows for a few optical

modes to propagate, we couple a TEM_{00} mode from free space into the ONF exciting one of the two degenerate HE_{11} quasi-linear fundamental modes. The structure of observed Rayleigh scattered light is consistent with this picture.

The probe and drive lasers are Toptica DLS pro. The transmission of the ONF at the drive and probe frequencies (780 nm and 852nm) is better than 84% including the coupling efficiency into and out of the ONF. The Balanced Photo Diode (BPD) is a Thorlabs PDB450A set to a gain of 10^5 . The MRs for the waveplates are Thorlab KPRM1E/M. To ensure that the polarization of the probe is balanced, we continuously look at BPD independent outputs in an auxiliary digital oscilloscope. If they show a difference for more than two trace widths we adjust (by less than 5 degrees) the half wave plate just before the analyzer PBS. We further amplify and filter the difference signal from BPD and observe no low frequency oscillations in the screen. For monitoring the difference output of the BPD in an oscilloscope we use a Stanford Research Systems SRS 560 low noise amplifier with gain of 50 and 10 kHz high pass and 300 kHz low pass 6 dB filters. To get the signal power spectrum, we send the difference signal from the BPD to a Rohde & Schwarz FSVA13 spectrum analyzer.

We have characterized the noise properties of the BPD and the spectrum analyzer. All numbers are for 1 Hz resolution and video bandwidths with a frequency around 190 kHz, the resonance frequency of the first torsional mode. The electronic noise on the spectrum analyzer is 7 nV, the electronic noise of the balanced detector is 15 nV. The photodetection of 60 μ W of probe power causes an increase in the noise level due to the light shot noise to 90 nV. We tested that this is

consistent with the expected shot noise by observing the square root relationship with the power.

To study the thermally induced noise in the torsional mode the measurements are done on resonance, with a typical resolution bandwidth <20 Hz, and video bandwidths of 1 Hz. A single drive scan for the amplitude measurements takes 36 seconds and we have averaged it 10 times. Although the data in Fig. 2 **b,c** are taken consecutively, amplitude first and the frequency shift next, there is a shift in time of the resonant frequency of about 20 Hz, consistent with other observations as the temperature of the laboratory is not sufficiently stable for the high sensitivity of the apparatus. For the data in Fig. 3, the torsional resonance shifts as the drive power increases (see Fig. 3 inset **a**), so we alternate measurements with and without drive to obtain statistics for the ratio (\pm one standard deviation of the mean).

We estimate the size of the rotation by using a typical voltage amplitude at the output of the BPD of $V_{AC} = 5 \mu\text{V}$ in the thermally excited fundamental torsional mode when the probe has an optical power of $P_{DC} = 60 \mu\text{W}$. This corresponds to a current of $i_{AC} = 5 \times 10^{-11}$ A (current to voltage gain of the BPD of 10^5), that with a responsivity of the detectors at the operating wavelengths of 0.5 A/W gives the optical power at the peak of $P_{AC} = 10^{-10}$ W. The assumptions that we make at this point are first that this optical power oscillating at the frequency of the first torsional mode is the result of the beat between the probe field E_{DC} and the rotating electric field E_R . Second, since the polarization rotation angle ϕ is small enough, we assume that $E_R = \phi E_{DC}$, which implies that the fiber rotates the angle of the electric field by its mechanical rotation. This gives $\phi = E_R E_{DC} / E_{DC}^2 = P_{AC} / P_{DC} = 10^{-10} / 6 \times 10^{-5}$, the ratio of the two optical powers,

estimating $\phi \approx 1.7 \times 10^{-6}$ rad.

Theoretical model We take the work of Wuttke ¹⁵ where there is a complete treatment of the torsional wave equation in Chapter 4 to justify our model. We look at a single mode, the fundamental. We follow the work of Saulson ³³ to find the spectral density of the thermal fluctuations of the mode.

The development of the model requires one further assumption. This is motivated by a previous work ¹⁶ where the probe polarization rotation was due to some inherent asymmetry in the nanofiber, mostly on the region where the waist connects to the tapers, as seen in figure 7 of Hoffman *et al.* ²⁷, which shows the profile of a microfiber constructed with the heat and pull method. This implies the oscillations that we see are from an effective thin waveplate, as all the other contributions from the length of the nanofiber cancel each other, given the symmetry of the first torsional mode with the ONF anchored at the two end points. Calculations based on the work of Wuttke ¹⁵ solving for the optical rotation of a slightly asymmetric fiber at the point where the taper begins confirm this.

The equation of motion (Langevin form) for the generalized coordinate (angle) with the torque in the direction of propagation for a thin disk is:

$$I\ddot{\theta}(t) + \gamma\dot{\theta}(t) + \kappa\theta(t) - A_0 \sin(2\theta(t)) = T_{\text{th}}, \quad (3)$$

where I is the moment of inertia of the ONF, γ is the damping coefficient, κ is the torsional spring constant, and T_{th} is the thermally induced torque that drives the system. The natural frequency of

the system is $\omega_0 = \sqrt{\kappa/I}$, and $A_0 = \frac{\epsilon E^2}{2\omega_l} \sin \Gamma$ is the coefficient that characterizes the amplitude of the driving torque, as in Eq. (1) due to the presence of the laser. T_{th} is a random torque with a white spectral density:

$$S_{T_{\text{th}}} = 4k_B T \gamma. \quad (4)$$

Without thermal excitation we can obtain the potential that generates the equations of motion:

$$U = U_0 + \frac{1}{2}\kappa\theta^2 + \frac{1}{2}A_0 \cos 2\theta. \quad (5)$$

We can neglect the constant term U_0 for the following discussion and consider

$$U - U_0 = \eta(\theta^2 + \frac{A_0}{\kappa} \cos 2\theta), \quad (6)$$

where η is the characteristic value of the undriven potential. A displacement of θ by $\pi/2$ will create an offset of the angle coordinate plus a constant term that can always be dropped out because it does not contribute to the equation of motion. This means that the only difference between the electric field aligned along the ordinary or extraordinary axis is the sign in front of the second term in the potential, i.e. the optomechanical potential. For light polarization angles close to the ordinary axis the problem is well approximated by a quartic potential with a larger effective torsional spring constant ($\kappa_{\text{eff}} = \kappa + 2A_0$). On the other hand, when the light is polarized near the extraordinary axis, for $A_0/\kappa > 1$ we obtain a (one-dimensional) symmetric double well potential, with two stability points away from $\theta = 0$. This quartic potential can have one or two minima, depending on the value of the optomechanical drive A_0 .

When we take only the first term in the expansion of the exerted torque we find the linear amplitude of the harmonic oscillator and its dependence on the parameters of the potential. On

resonance, if the Q factor is large enough, we have $\omega_0 = (\kappa - 2A_0)/I$. For a torque amplitude of T_{th} , obtained from the spectral density in equation 4, we can write:

$$\theta(\omega) = \frac{T_{\text{th}}}{(\kappa - 2A_0) - I\omega^2 + i\gamma\omega}. \quad (7)$$

Then the absolute value squared on resonance gives:

$$\theta(\omega)^2 = \frac{\langle T_{\text{th}}^2 \rangle}{\omega_0^2 \gamma^2} = \frac{4k_B T}{\omega_0^2 \gamma}, \quad (8)$$

where $\langle T_{\text{th}}^2 \rangle = S_{T_{\text{th}}}$ corresponds to the delta correlation of the random torque T_{th} , with a spectral density given by Eq. (4).

We need to look at the equation for the fluctuations around the steady state of Eq. (3).

The steady state of equation 3 at zero temperature satisfies:

$$\theta_{ss} = \frac{A_0 \sin 2\theta_{ss}}{\kappa}. \quad (9)$$

The linearized differential equation for a perturbation $\delta\theta$ is then:

$$I\ddot{\delta\theta}(t) + \gamma\dot{\delta\theta}(t) + \delta\theta(t) [\kappa - A_0 \cos(2\theta_{ss})] = T_{\text{th}}. \quad (10)$$

This equation depends on the steady state angle. So the result for the steady state oscillation frequency ω_{ss} is

$$\omega_{ss} = \sqrt{\frac{\kappa - A_0 \cos 2\theta_{ss}}{I}}. \quad (11)$$

We can find a small shift in the frequency due to the perturbation:

$$\delta\omega = -\sqrt{\frac{\kappa}{I}} \left(\frac{A_0 \cos 2\theta_{ss}}{2\kappa} \right). \quad (12)$$

The fluctuating amplitude of the angle $\delta\theta$, on top of θ_{ss} , is then

$$\delta\theta = \frac{T_{\text{th}}/I}{\gamma\sqrt{(\kappa - A_0 \cos 2\theta_{ss})/I}}, \quad (13)$$

from which we obtain the spectral density of the system as in Eq. (2).

The numerical solution of the full differential equation 3 shows the validity of the approximation as long as the size of the perturbation $\delta\theta$ is less than 0.5 of the steady state.

Data Availability The data that support the findings of this study are available from the authors upon reasonable request.

1. J. H. Poynting. The wave motion of a revolving shaft, and a suggestion as to the angular momentum in a beam of circularly polarised light. *Proc. R. Soc. Lond. A*, 82:557, 1909.
2. Richard A. Beth. Direct detection of the angular momentum of light. *Phys. Rev.*, 48:471–471, Sep 1935.
3. Richard A. Beth. Mechanical detection and measurement of the angular momentum of light. *Phys. Rev.*, 50:115–125, Jul 1936.
4. A. H. S. Holbourn. Angular momentum of circularly polarised light. *Nature*, 137(3453):31–31, 1936.

5. H Shi and M Bhattacharya. Optomechanics based on angular momentum exchange between light and matter. *Journal of Physics B: Atomic, Molecular and Optical Physics*, 49(15):153001, jun 2016.
6. M. E. J. Friese, T. A. Nieminen, N. R. Heckenberg, and H. Rubinsztein-Dunlop. Optical alignment and spinning of laser-trapped microscopic particles. *Nature*, 394(6691):348–350, 1998.
7. M. E. J. Friese, T. A. Nieminen, N. R. Heckenberg, and H. Rubinsztein-Dunlop. Erratum: Optical alignment and spinning of laser-trapped microscopic particles. *Nature*, 395(6702):621–621, 1998.
8. Thai M. Hoang, Yue Ma, Jonghoon Ahn, Jaehoon Bang, F. Robicheaux, Zhang-Qi Yin, and Tongcang Li. Torsional optomechanics of a levitated nonspherical nanoparticle. *Phys. Rev. Lett.*, 117:123604, Sep 2016.
9. René Reimann, Michael Doderer, Erik Hebestreit, Rozenn Diehl, Martin Frimmer, Dominik Windey, Felix Tebbenjohanns, and Lukas Novotny. GHz rotation of an optically trapped nanoparticle in vacuum. *Phys. Rev. Lett.*, 121:033602, Jul 2018.
10. Jasper Chan, T. P. Mayer Alegre, Amir H. Safavi-Naeini, Jeff T. Hill, Alex Krause, Simon Gröblacher, Markus Aspelmeyer, and Oskar Painter. Laser cooling of a nanomechanical oscillator into its quantum ground state. *Nature*, 478:89, Oct 2011.
11. Uroš Delić, Manuel Reisenbauer, David Grass, Nikolai Kiesel, Vladan Vuletić, and Markus Aspelmeyer. Cavity cooling of a levitated nanosphere by coherent scattering. *Phys. Rev. Lett.*, 122:123602, Mar 2019.

12. Nils T. Otterstrom, Ryan O. Behunin, Eric A. Kittlaus, and Peter T. Rakich. Optomechanical cooling in a continuous system. *Phys. Rev. X*, 8:041034, Nov 2018.
13. Markus Aspelmeyer, Tobias J. Kippenberg, and Florian Marquardt. Cavity optomechanics. *Rev. Mod. Phys.*, 86:1391–1452, Dec 2014.
14. C. Wuttke, G. D. Cole, and A. Rauschenbeutel. Optically active mechanical modes of tapered optical fibers. *Phys. Rev. A*, 88:061801, Dec 2013.
15. Christian Wuttke. *Thermal excitations of optical nanofibers measured with a cavity*. PhD thesis, University of Mainz, 2014.
16. Eliot F. Fenton, Adnan Khan, Pablo Solano, Luis A. Orozco, and Fredrik K. Fatemi. Spin-optomechanical coupling between light and a nanofiber torsional mode. *Opt. Lett.*, 43(7):1534–1537, Apr 2018.
17. George Y. Chen, Ming Ding, Trevor P. Newson, and Gilberto Brambilla. A review of microfiber and nanofiber based optical sensors. *The Open Optics Journal*, 7:(Suppl–1, M3) 32–57, 2013.
18. P. Solano, J. A. Grover, J. E. Hoffman, S. Ravets, F. K. Fatemi, L. A. Orozco, and S. L. Rolston. *Advances in Atomic Molecular and Optical Physics*, volume 46, chapter Optical Nanofibers: A New Platform for Quantum Optics, pages 355–403. Academic Press, 2017.
19. V.B. Braginsky and S.P. Vyatchanin. Low quantum noise tranquilizer for Fabry-Perot interferometer. *Physics Letters A*, 293(5):228 – 234, 2002.

20. Thomas Corbitt, Yanbei Chen, Edith Innerhofer, Helge Müller-Ebhardt, David Ottaway, Henning Rehbein, Daniel Sigg, Stanley Whitcomb, Christopher Wipf, and Nergis Mavalvala. An all-optical trap for a gram-scale mirror. *Phys. Rev. Lett.*, 98:150802, Apr 2007.
21. E. E. Wollman, C. U. Lei, A. J. Weinstein, J. Suh, A. Kronwald, F. Marquardt, A. A. Clerk, and K. C. Schwab. Quantum squeezing of motion in a mechanical resonator. *Science*, 349(6251):952–955, 2015.
22. J.-M. Pirkkalainen, E. Damskägg, M. Brandt, F. Massel, and M. A. Sillanpää. Squeezing of quantum noise of motion in a micromechanical resonator. *Phys. Rev. Lett.*, 115:243601, Dec 2015.
23. Muddassar Rashid, Tommaso Tufarelli, James Bateman, Jamie Vovrosh, David Hempston, M. S. Kim, and Hendrik Ulbricht. Experimental realization of a thermal squeezed state of levitated optomechanics. *Phys. Rev. Lett.*, 117:273601, Dec 2016.
24. Li He, Huan Li, and Mo Li. Optomechanical measurement of photon spin angular momentum and optical torque in integrated photonic devices. *Science Advances*, 2(9), 2016.
25. H. He, M. E. J. Friese, N. R. Heckenberg, and H. Rubinsztein-Dunlop. Direct observation of transfer of angular momentum to absorptive particles from a laser beam with a phase singularity. *Phys. Rev. Lett.*, 75:826–829, Jul 1995.
26. S. K. Selvaraja and P. Sethi. *Emerging Waveguide Technology*, chapter Review on Optical Waveguide. IntechOpen, 2018.

27. J. E. Hoffman, S. Ravets, J. A. Grover, P. Solano, P. R. Kordell, J. D. Wong-Campos, L. A. Orozco, and S. L. Rolston. Ultrahigh transmission optical nanofibers. *AIP Advances*, 4(6):067124, June 2014.
28. S Ravets, J E Hoffman, L A Orozco, S L Rolston, G Beadie, and F K Fatemi. A low-loss photonic silica nanofiber for higher-order modes. *Opt. Express*, 21(15):18325–35, July 2013.
29. Maxime Joos, Alberto Bramati, and Quentin Glorieux. Complete polarization control for a nanofiber waveguide using the scattering properties. *Opt. Express*, 27(13):18818–18830, Jun 2019.
30. Pablo Solano, Fredrik K. Fatemi, Luis A. Orozco, and Steven L. Rolston. Dynamics of trapped atoms around an optical nanofiber probed through polarimetry. *Opt. Lett.*, 42(12):2283–2286, March 2017.
31. S. Chakram, Y. S. Patil, L. Chang, and M. Vengalattore. Dissipation in ultrahigh quality factor sin membrane resonators. *Phys. Rev. Lett.*, 112:127201, Mar 2014.
32. P. H. Kim, B. D. Hauer, T. J. Clark, F. Fani Sani, M. R. Freeman, and J. P. Davis. Magnetic actuation and feedback cooling of a cavity optomechanical torque sensor. *Nature Communications*, 8(1):1355, 2017.
33. Peter R. Saulson. Thermal noise in mechanical experiments. *Phys. Rev. D*, 42:2437–2445, Oct 1990.